# Photodegradation of Methylene Blue (MB) using Cerium-doped Zinc Oxide nanoparticles

SHANTHI KARIDAS[1,*], B KALYANI VEENA[1], NAVNEETHA PUJARI[1], POTHARAJU KRISHNA[2] and VARDHANI CHUNDURU[2]

[1] Department of Physics, College for Women, Osmania University, Hyderabad, India
[2] Department of Physics, Osmania University, Hyderabad, India
e-mail: shanthikaridas@gmail.com

**Abstract.** Cerium-doped Zinc Oxide nanoparticles were prepared with co-precipitation method. X-Ray diffraction (XRD) analysis shows sharp peaks conforming the crystalline nature of prepared particles. Crystallite size was found from XRD peaks. A Field Emission Scanning Electron Microscope (FESEM) was used to see the particles and hexagonal shape. Spectroscopic properties were studied using a Fourier Transform-Infra Red (FT-IR) spectrometer and Raman spectrometer. Optical properties were studied using a Diffuse Reflectance Ultraviolet Visible (DRS UV–VIS), spectrophotometer. Band gap of doped particles reduces as doping concentration increases. Reduced band gap of Cerium doped particles makes them a good catalyst. There are many organic dyes which are used as coloring agents by industries like textile, printing, etc. These industries release harm full pollutants into water bodies, which effect human and aquatic life. Prepared Cerium-doped ZnO nanoparticles have proved to photodegrade Methylene Blue. Undoped ZnO nanoparticles decolorized the solution in 210 min with 81.93% efficiency. Ce (0.03 wt%) doped ZnO nanoparticles decolorized the solution in 120 min with 92.62% efficiency.

**Keywords.** Zinc Oxide nanoparticles; cerium; crystallite size; band gap; Methylene Blue.

## 1. Introduction

The nanoparticles of Zinc Oxide (ZnO) are one of the most studied materials. Doping of ZnO nanoparticles is one effective way to improve the properties for various applications. In particular, doping ZnO with rare earth materials is of interest in tailoring its optical properties [1]. Zinc and Oxygen vacancies have low formation energy than other defects such as Zinc and Oxygen interstitials. Depending on condition Oxygen vacancies can act as electron donor sites by releasing trapped electrons, thereby causing high conductivity and n-type semiconductor behavior, these defects have strong influence on optical properties, especially luminescence. When ZnO nanoparticles are doped with rare earth elements, there is change in structural, optical and magnetic properties.

Rare earth doped ZnO nanoparticles have several applications in flat panel displays, solar cells, solid state lighting, spintronics, gas sensing, photocatalyst, etc.

Aisah *et al*. have shown that band gap energy of undoped ZnO nanorods was 3.23 eV and decreased to 3.18 eV after Ce doping [2]. According to Clament Sagaya Selvam *et al.*, the Oxygen defects are proposed to be the active sites of the ZnO photocatalyst. Among the catalysts, 1.5 wt% Ce-doped ZnO showed superior performance towards degradation and mineralization of nonylphenol than other doped ZnO and pure ZnO [3].

Cerium (Ce)-doped Zinc Oxide nanoparticles can be effectively used as photocatalyst by tuning its band gap. Compared to undoped ZnO nanoparticles, Cerium-doped ZnO nanoparticles band gap reduces due to creation of extra energy levels. Undoped ZnO is photoactive in the near UV areas; so, only 3–4% of solar light is utilized. Therefore, simultaneous surface modification and doping of ZnO nanoparticles not only changes the surface morphology, size and surface charges of the nanoparticles synthesized, but also significantly shifts the band gap energy to the visible region, where utilization of solar light is more comparable to that of the UV region [4] Gunasekaran et al prepared Cerium-doped ZnO nanoparticles by co-precipitation method using a capping agent. He has shown that band gap reduces from 3.02 eV to 2.71 eV with increasing Ce concentration. He also has shown that Cerium-doped ZnO nanoparticles can be efficiently used to photodegrade organic dye Methylene Blue (MB). For 0.07% of Cerium he has got highest efficiency.

---

*For correspondence

In the present work Cerium-doped ZnO nanoparticles with different concentrations were prepared with co-precipitation method without using any capping agent. Structural and optical properties were studied for the prepared particles. Then Cerium-doped ZnO nanoparticles were efficiently used to photodegrade organic dye MB. These organic dyes are released in to water streams by textile, food, printing industries, etc. The dye polluted water is harmful for aquatic life and is carcinogenic to human beings [5]. Hence the treatment of polluted water is of utmost importance.

## 2. Experimental procedure

### 2.1 *Synthesis of Cerium-doped ZnO nanoparticles*

All the Chemicals, Zinc Nitrate Hexa hydrate $Zn(No_3)_2 \cdot 6H_2o$, Cerium Nitrate Hexa hydrate $Ce(No_3)_3 \cdot 6H_2o$, Sodium hydroxide pellets were purchased from Central Drug House, New Delhi. Cerium-doped ZnO nanoparticles at various concentrations were prepared with modified co-precipitation method using equation $Zn_{(1-x)}Ce_xO$. Where 'x' varies as x = 0, 0.01, 0.03, 0.05, 0.07, 0.09, 0.1 weight % of Cerium. The particles were named as, undoped ZnO, ZnOCe1, ZnOCe2, ZnOCe3, ZnOCe4, ZnOCe5, ZnOCe6, respectively. $Zn(No_3)_2 \cdot 6H_2O$ and $Ce(No_3)_3 \cdot 6H_2o$ were added to deionised water in stoichiometric ratios. The solution was thoroughly mixed with a magnetic stirrer. Sodium hydroxide pellets were added till the pH of the solution became ∼ 12. Upon continuous stirring white precipitate was formed. The solution was washed several times to remove impurities. Then the Powder was kept in hot air oven, overnight, to make it dry powder. Dried powder was grinded. The grinded nanoparticles were sintered conventionally at 600 °C for 2 h. Then characterised with XRD, FESEM, and FTIR. To study optical properties RAMAN, UV_VIS absorption analysis was done. There are no secondary phases seen in the XRD analysis of the 0.01, 0.03 wt% of rare earth doping in ZnO nanoparticles. Hence photodegradation of (MB) was studied using x = 0.03 wt % of Ce, doped and undoped ZnO nanoparticles.

### 2.2 *Photodegradation experimental procedure*

Photocatalyst (1 g) was added to 200 ml aqueous solution of 0.25 mM Methylene Blue. The solution was kept on a magnetic stirrer in dark for 30 min to obtain equilibrium state. Then the solution was exposed to sunlight. After every 10 min of exposure to sunlight solution was collected and centrifuged for 10 min. Samples were collected for 10 min, 20 min, 30 min, and 40 min of exposure to sunlight and after complete decolorization of solution. Absorbance was studied using a UV–VIS spectrophotometer.

Photodegradation percentage was calculated using Eq. (1).

$$Photodegradation \% = ((A_0 - A_t)/A_0) \times 100 \quad (1)$$

where $A_0$ is absorbance at 0 min, and $A_t$ is absorbance at regular time intervals of 10, 20, 30, and 40 min of exposure to sunlight.

## 3. Characterisation

Structural analysis of the Ce-doped ZnO nanoparticles was studied using a Rigaku Ultima IV X-Ray Difractometer (XRD) with Cu target and $k_\alpha$ radiation having 1.5418 Å wavelength in the range 20° to 80°. The morphology was studied using Gemini 500 FESEM. Spectroscopic properties were studied using a Jasco 4200 FTIR spectrometer. Raman spectra were recorded by WITEC Alpha 300 using 633 nm laser source. Optical properties were studied using a Jasco V-670 Diffuse Reflectance UV–VIS spectrophotometer. Photodegradation absorbance was studied using a UV–VIS spectrophotometer from Agilent Technologies, model no cary 60.

## 4. Results and discussion

### 4.1 *X-ray diffraction analysis*

The X-Ray Diffraction analysis of the undoped and Ce-doped ZnO nanoparticles is shown in Fig. 1. The sharp peaks show that the formed nanoparticles are crystalline in nature. The angles obtained at 31°, 34°, 36°, 47°, 56°, 62°, 66°, 67°, and 69° are in accordance with JCPDS card (36–1451) and confirm that formed particles are ZnO nanoparticles. Powd software was used to index the peaks with h, k, l values. A secondary phase peak at $2\theta = 28°$ corresponds to $CeO_2$ .When Ce is doped into
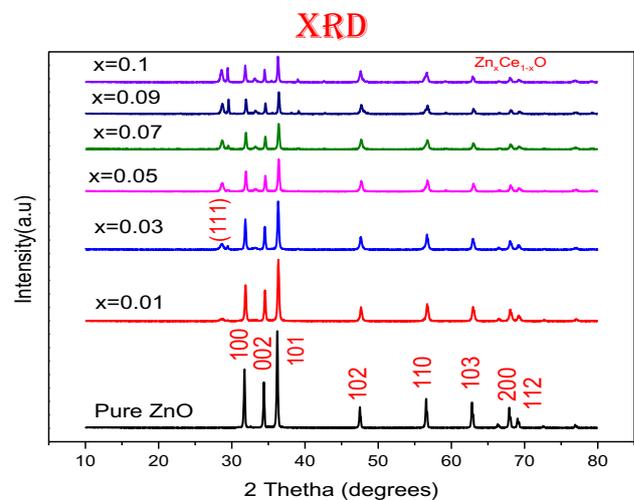


**Figure 1.** XRD pattern of undoped and Ce-doped ZnO nanoparticles.

**Table 1.** Values of lattice parameters 'a', 'c', X-Ray density, Crystallite size, Strain with varying Ce concentrations
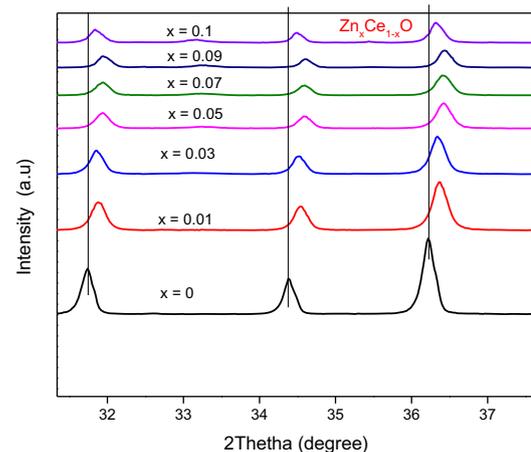
| Sl.No | Sample name | Cerium concentration | Lattice parameter 'a' (A°) | Lattice parameter 'c' (A°) | True density g/cm³ | Crystallite size (nm) | Lattice strain $\varepsilon$ | c/a |
|---|---|---|---|---|---|---|---|---|
| 1 | Pure ZnO | X = 0 | 3.254 | 5.209 | $1.697 \times 10^{-23}$ | 51.89 | 0.0044 | 1.6007 |
| 2 | ZnOCe1 | X = 0.01 | 3.243 | 5.190 | $1.736 \times 10^{-23}$ | 40.03 | 0.0057 | 1.06001 |
| 3 | ZnOCe2 | X = 0.03 | 3.244 | 5.193 | $1.765 \times 10^{-23}$ | 42.03 | 0.0055 | 1.6008 |
| 4 | ZnOCe3 | X = 0.05 | 3.237 | 5.183 | $1.808 \times 10^{-23}$ | 39.66 | 0.0058 | 1.6009 |
| 5 | ZnOCe4 | X = 0.07 | 3.236 | 5.182 | $1.841 \times 10^{-23}$ | 38.73 | 0.0059 | 1.6013 |
| 6 | ZnOCe5 | X = 0.09 | 3.237 | 5.181 | $1.873 \times 10^{-23}$ | 49.45 | 0.0046 | 1.6007 |
| 7 | ZnOCe6 | X = 0.1 | 3.246 | 5.196 | $1.873 \times 10^{-23}$ | 47.50 | 0.0048 | 1.6008 |
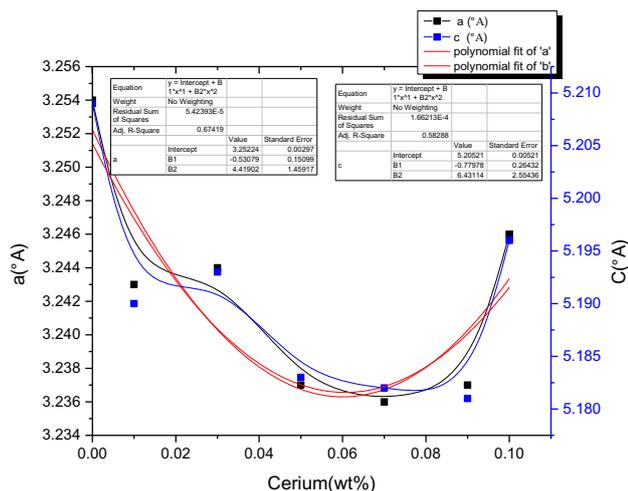


**Figure 2.** Variation of Lattice Parameters 'a', 'c' with Ce concentration.



**Figure 3.** Magnified XRD image in 2 theta range from 20 ° to 40 °.

ZnO, all of the Ce do not go in to the solid solution, but some of the Ce forms impurity phase $CeO_2$. Crystallite size was calculated using Debye Scherer equation and was found to be in the range of 38–51 nm. As Zinc Oxide has hexagonal unit cell with wurzite structure, the lattice parameters 'a', 'c' were calculated, along with strain, volume, true density and are tabulated in table 1. Due to increased strain the lattice parameters decrease anisotropically. As the concentration of Ce increases in prepared ZnO nanoparticles the true density increases, showing that Ce atoms have been doped into the nanoparticles. Figure 2 shows the variation of lattice parameters with varying Ce concentration. The magnified XRD graph in the 2θ range 30–40° is shown in Fig. 3. Due to strain, for all the concentrations the peaks shift towards higher angle side correspondingly lattice parameters decrease.

### 4.2 *FESEM*

FESEM images of undoped and Ce-doped ZnO nanoparticles are shown in figures 4, 5. The FESEM pictures were taken at 200 nm scale. Hexagonal shape of undoped ZnO particles is clearly visible. As the Ce concentration increases, there is change in shape, grain size and agglomeration increases due to nucleation of Ce ions [6].

### 4.3 *FTIR spectra*

Chemical composition of the prepared ZnO nanoparticles was analyzed using a FT-IR spectrometer. Figure 6 shows the absorption peaks of pure and doped ZnO nanoparticles. The peaks are observed at 1384, 831, 478 $cm^{-1}$. The absorption peak at 3449 $cm^{-1}$ corresponds to O–H stretching vibration. The peak at 1384 $cm^{-1}$ corresponds to C-O stretching mode. The Ce–O bond is present at 831$cm^{-1}$, this peak is observed in only doped particles, showing that Ce has been doped into ZnO NP's. Peak at 478 $cm^{-1}$ corresponds to Zn–O stretching mode.

### 4.4 *Raman analysis*

Raman spectra were taken only for samples undoped ZnO, ZnOCe1, ZnOCe3, and ZnOCe6 with 0.5 s integration time.
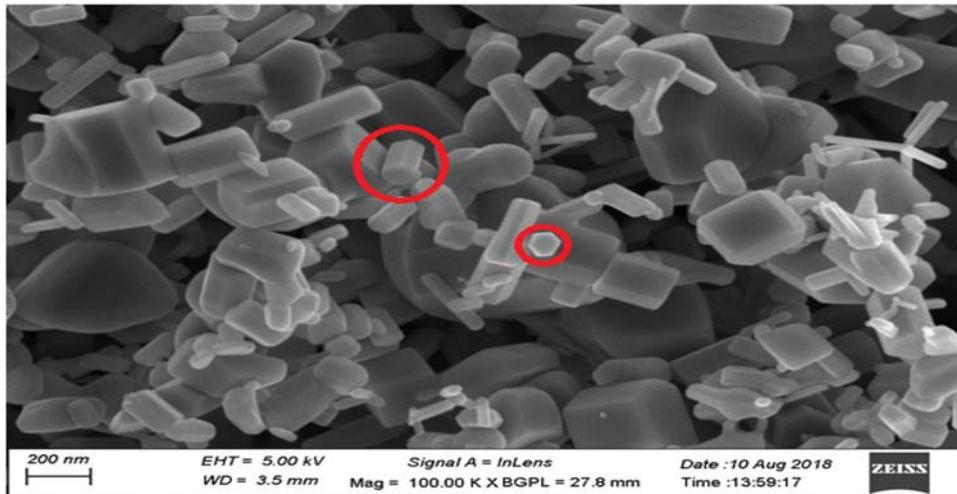
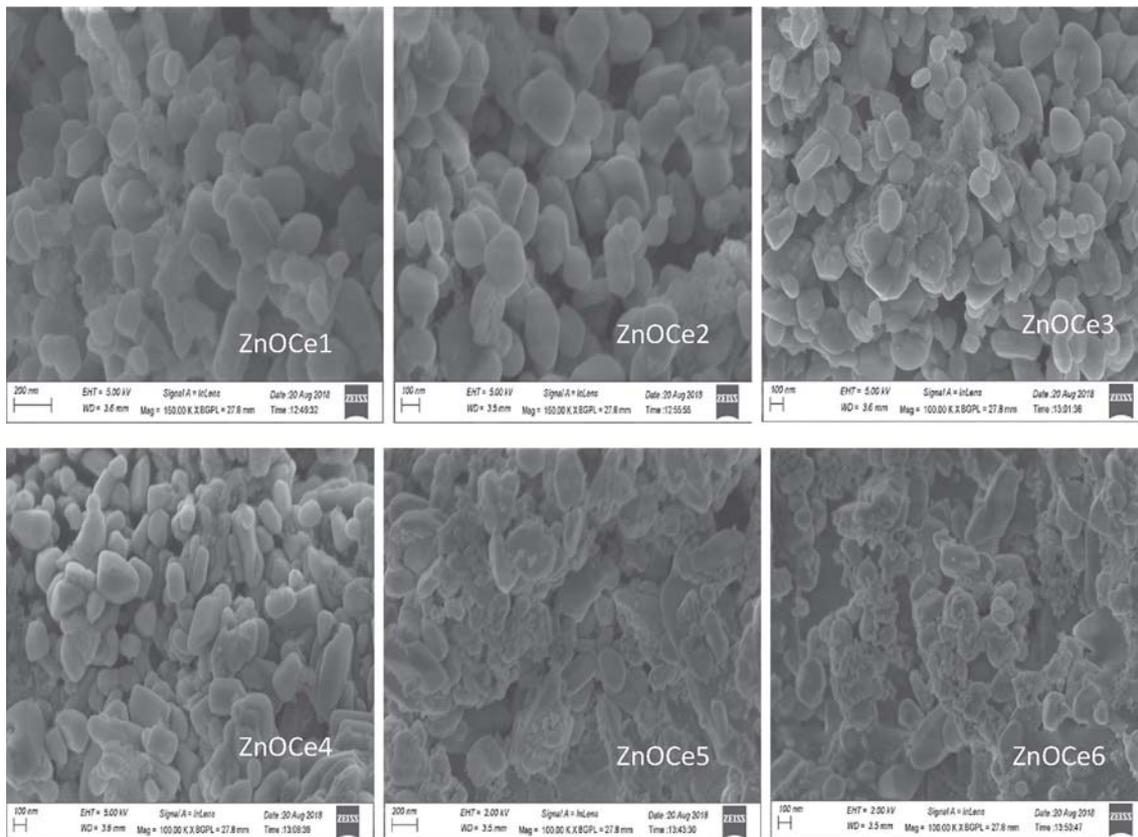**Figure 4.** FESEM picture of undoped ZnO nanoparticles.



**Figure 5.** FESEM pictures of Cerium doped ZnO nanoparticles at 0.01%,0.03%,0.05%,0.07%,0.09%,0.1% percentage of Cerium respectively.

Two peaks were observed at 331 cm$^{-1}$ and 434 cm$^{-1}$ for pure ZnO NPs corresponding to E$_2$M and E$_2$H mode respectively. E$_2$H mode is characteristic of the Wurzite lattice and indicates good crystalline nature. For sample ZnOCe1 the Peaks are observed at 331 cm$^{-1}$, 432 cm$^{-1}$ and a new peak at 462 cm$^{-1}$. The E$_2$H peak is red shifted
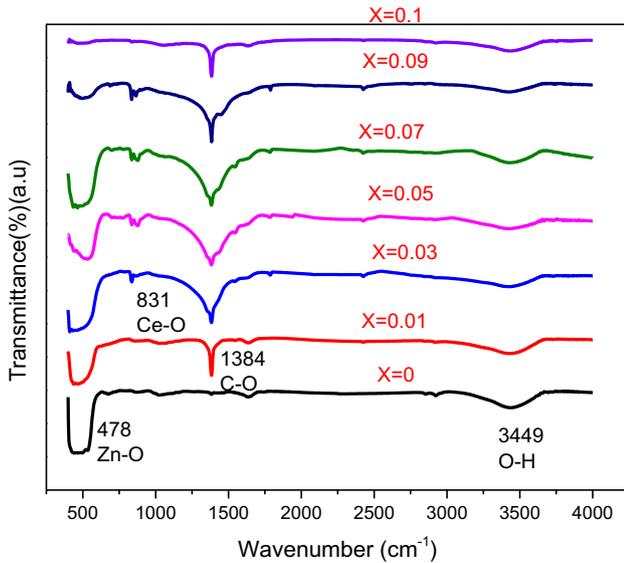
**Figure 6.** FTIR spectra of undoped and Cerium-doped ZnO nanoparticles at various concentrations.
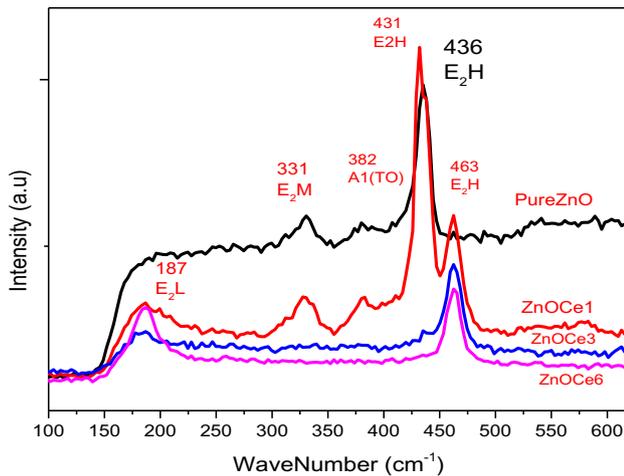


**Figure 7.** Raman spectra of undoped and Cerium-doped ZnO nanoparticles at various concentrations.



**Figure 8.** UV-VIS absorbance graph of undoped and Ce-doped ZnO nanoparticles at various concentrations.
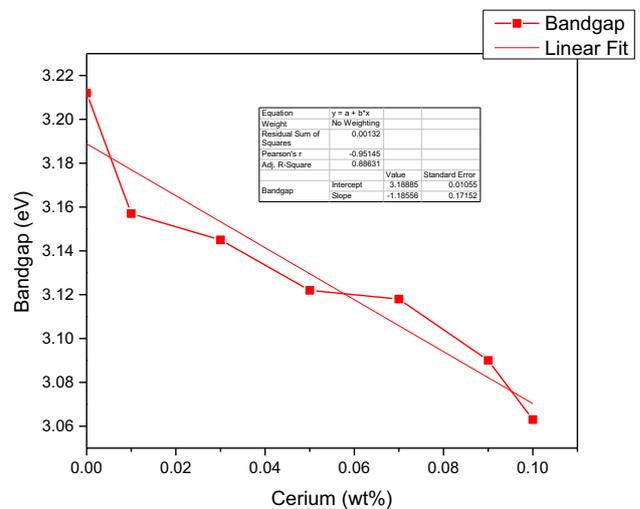


**Figure 9.** Variation of band gap with increasing Ce concentration.

$2 cm^{-1}$. Generally the three possible mechanisms that may be responsible for the observed phonon peak shifts in the corresponding Raman spectra are (1) Spatial confinement within the nanoparticle boundaries. (2) Phonon localization by defects such as Oxygen deficiency, Zinc excess, surface impurities, etc. (3) Laser-induced heating in nanostructure ensembles and tensile strain [7]. For samples ZnOCe3, ZnOCe6 peak is observed at only 462 $cm^{-1}$. The signal observed at 457 $cm^{-1}$ originates from the Raman active mode of Cerium Oxide [8]. The absence of $E_1(LO)$ peak at 588 $cm^{-1}$ related to oxygen deficiency indicates that the prepared ZnO nanoparticles are of good optical quality [9]. (Fig. 7)
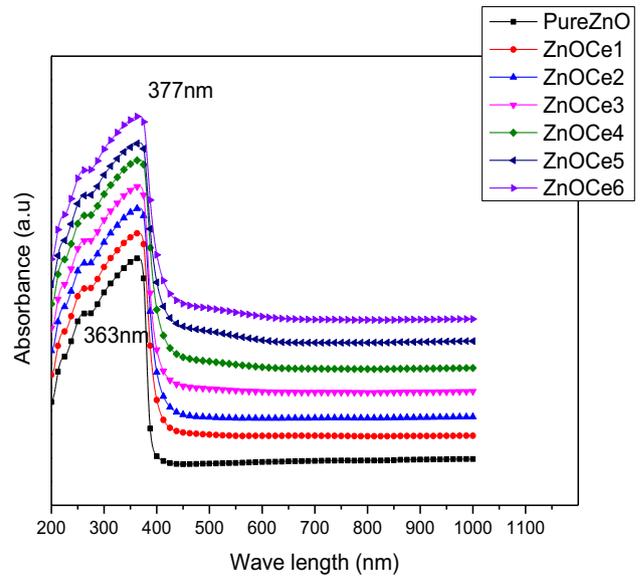
### 4.5 *Diffuse reflectance UV–VIS absorption analysis*

Figure 8 shows the Diffuse Reflectance UV absorption graph of pure and Ce doped ZnO NP's, Sharp absorption Peak is Observed at 363 nm for pure ZnO nanoparticles and 377 nm for x=0.1, Ce doped ZnO nanoparticles. As the Ce concentration increases the peak shifts towards higher wavelength side. Band gap '$E_g$' was calculated using (2).

$$(\alpha h v)^2 = k(h v - E_g) \qquad (2)$$

where '$\alpha$' is absorption coefficient, 'h' is Planck's constant, '$E_g$' is band gap, 'K' some constant, '$v$' is frequency.

**Figure 10.** Color change in the MB solution by undoped Zinc Oxide nanoparticles after exposure to sunlight.



**Figure 11.** UV-VIS absorbance spectra of undoped Zinc Oxide nanoparticles for different time intervals of exposure to sunlight.

Extrapolation of the Tauc plot between $(\alpha h\nu)^2$ and $h\nu$ gives the band gap.

The band gap value for pure ZnO NP's is 3.212 eV. For Ce doped nanoparticles the band gap values are 3.157, 3.145, 3.122, 3.118, 3.090, 3.063 eV for 0.01, 0.03, 0.05, 0.07, 0.09, 0.1 concentrations of Cerium respectively. Figure 9 shows the variation of band gap with Ce concentration. As expected the band gap of the doped particles reduced due to the creation of extra levels in the band gap. Hence particles can be efficiently used as photocatalysts.

## 5. Photodegradation of Methylene Blue

### 5.1 *Photodegradation of Methylene Blue with undoped Zinc Oxide nanoparticles*

Undoped ZnO nanoparticles were used as photocatalyst to photodegrade Methylene Blue following the procedure mentioned above. Figure 10 shows the solution kept in
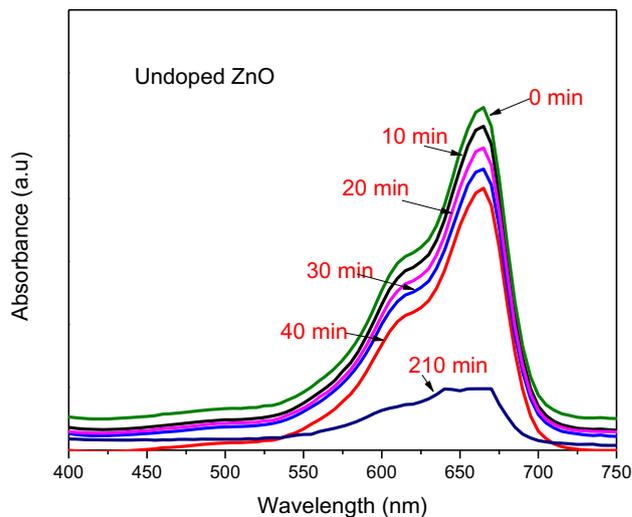
sunlight. De colorization of the solution can be seen. In 210 min (3 and 1/2 h) undoped ZnO particles completely de colorized the Methylene Blue solution with 81% efficiency. Figure 11 shows the absorbance vs. wavelength graph for different time intervals of exposure to sunlight. As the exposure time increases, absorbance decreases showing that undoped ZnO nanoparticles act as good photocatalyst. Table 2 gives absorbance values at 663 nm where absorbance is maximum. From first 40 min it can be seen that absorbance decreases and decolorization starts, hence the next absorbance value is taken after complete decolorization.

Photocatalytic oxidation steps can be explained in the following steps. Organic pollutants diffuse from the liquid phase to the surface of Zinc Oxide, then organic pollutants are adsorbed on the surface of ZnO, oxidation and reduction reactions in the adsorbed phase, desorption of the products, removal of the products from the interface region [10] (Fig. 12).

### 5.2 *Photodegradation of Methylene Blue with Cerium doped Zinc Oxide nanoparticles*

Photodegradation of Methylene Blue experiment was done with Cerium doped ZnO nanoparticles. Figure 13 shows color change in the MB solution by Ce(x = 0.03 wt%) doped ZnO nanoparticles after exposure to sunlight. Figure 14 shows absorbance spectra of Cerium doped Zinc Oxide nanoparticles for different time intervals of exposure to sunlight. From graph it can be seen that Cerium doped Zinc Oxide nanoparticles act as good photocatalyst to degrade Methylene Blue with 92% efficiency for Ce( x = 0.03 wt%). Table 3 gives absorbance values at 663 nm and photodegradation % and Ce(0.03 wt%). The possible
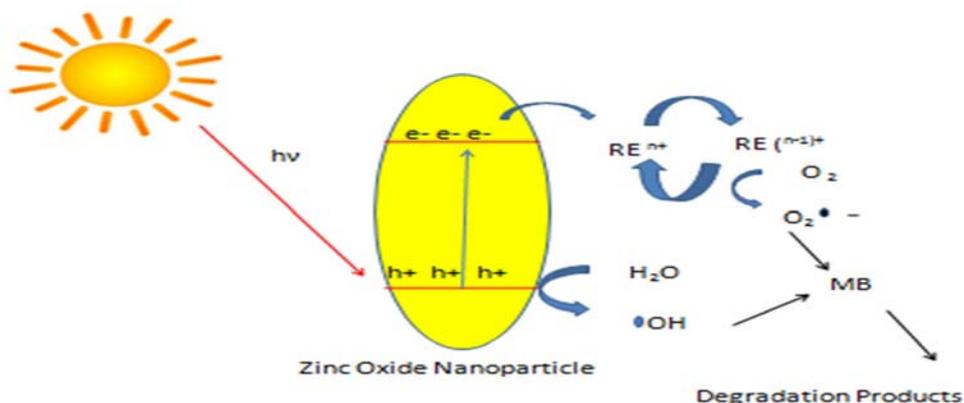
**Figure 12.**  Photodegradation mechanism.

**Table 2.** Absorbance and Photodegradation % of ZnO nanoparticles for different time intervals of exposure to sunlight

| Time of sunlight exposure | Absorbance at 663 nm | Photodegradation % |
|---|---|---|
| 0 min | 0.548 | |
| 10 min | 0.512 | 6.56 |
| 20 min | 0.482 | 12.04 |
| 30 min | 0.446 | 18.61 |
| 40 min | 0.415 | 24.27 |
| 210 min | 0.099 | 81.93 |

mechanism is explained as follows. When Cerium doped Zinc Oxide nanoparticles in MB solution is exposed to sunlight, photons are absorbed and electrons are excited from valence band to conduction band. $Ce^{4+}$ ions get reduced to $Ce^{3+}$ by taking photo excited electrons, thereby inhibiting $e-/h+$ recombination. $Ce^{3+}$ ions get oxidized by reacting with dissolved $O_2$ to generate superoxide anions and thus regenerate $Ce^{4+}$ ions. Meanwhile, the holes in the valence band of ZnO react with water to produce hydroxyl radicals. The $O_2^{\cdot-}$, $\cdot$OH and h+ species degrade MB to final products [11].

## 5.3 *Photodegradation efficiency*

Photodegradation efficiency of semiconductors depends on many factors like phase structure, surface hydroxyl groups, particle size, surface defects, etc. [12]. Photodegradation efficiency was calculated with Eq. (1) at 663 nm where the absorbance is maximum. Figure 15 shows photodegradation percentage graph till 40 min of exposure to sunlight for undoped and 0.03wt% of Cerium doped ZnO nanoparticles. It can be inferred from graph that as the sunlight exposure time increases degradation percentage increases. Cerium doped Zinc Oxide nanoparticles have highest efficiency than undoped Zinc Oxide nanoparticles. Particle Size has direct influence on photodegradation efficiency, as surface



**Figure 13.**  Color change in the MB solution by Ce(x = 0.03 wt%) doped ZnO nanoparticles after exposure to sunlight.

area is more for small particles. With reduced band gap and less particle size, Ce (0.03 wt%) stands out to be the best material for photodegradation. Table 4 summarizes the efficiencies when complete decolorization has taken place.
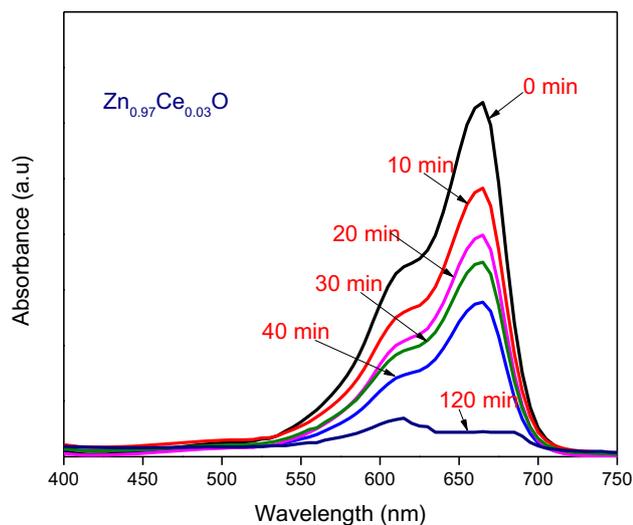
**Figure 14..** UV-VIS absorbance spectra of 0.03 wt% of Ce doped ZnO nanoparticles for different time intervals of exposure to sunlight.

**Table 3..** Absorbance and photodegradation % of Cerium (0.03%) Zinc Oxide nanoparticles for different time intervals of exposure to sunlight

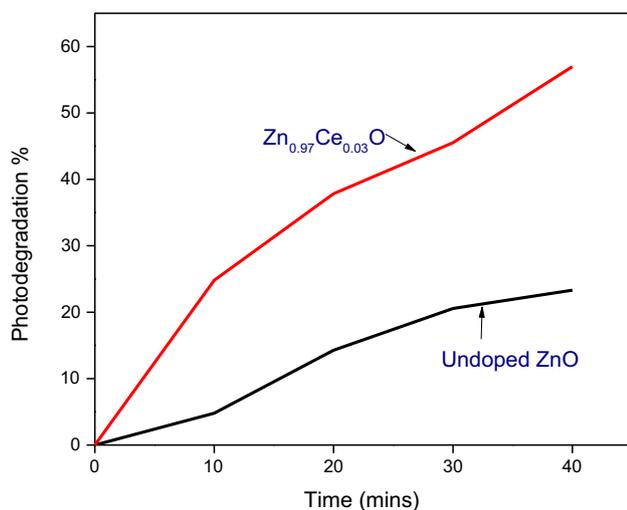| Time of sunlight exposure | Absorbance at 663 nm | Photodegradation % |
|---|---|---|
| 0 min | 0.637 | |
| 10 min | 0.483 | 24.1 |
| 20 min | 0.396 | 37.83 |
| 30 min | 0.344 | 45.99 |
| 40 min | 0.277 | 56.51 |
| 120 min | 0.047 | 92.62 |



**Figure 15.** Photodegradation percentage of MB with undoped and 0.03 wt% of Ce doped ZnO nanoparticles.

**Table 4.** Photodegradation efficiencies of samples when complete decolorization has taken place

| Sample name | Time taken for decolorization | Photodegradation efficiency (%) |
|---|---|---|
| Undoped ZnO | 210 min | 81.93 |
| $Zn_{0.97}Ce_{0.03}O$ | 120 min | 92.62 |

## 6. Conclusion

Undoped ZnO nanoparticles and Cerium doped ZnO nanoparticles have been prepared by co-precipitation method. XRD analysis reveals the crystalline nature of doped ZnO nanoparticles. The crystallite size of Ce doped decreased compared to undoped ZnO nanoparticles. FESEM pictures show the hexagonal shape. The grain size of Ce doped nanoparticles increases as concentration increases. FT-IR analysis shows the absorption peak at $478 cm^{-1}$ corresponding to Zn-O stretching. Ce-O absorption peak is obtained at $831 cm^{-1}$. Raman analysis of prepared nanoparticles shows $2E_2M$ and $2E_2H$ modes. DRS UV-VIS plot shows strong absorption peak at 363 nm. Decrease in band gap with Ce doping shows that doped ZnO nanoparticles can be used for photodegradation and hence acts good photocatalysts. Photodegradation of Methylene Blue was done using undoped and Ce doped ZnO nanoparticles. For all the doped and undoped ZnO nanoparticles absorbance decreases in the visible region, as the sunlight exposure time increases. Photodegradation efficiency was calculated at 663 nm where the absorbance is maximum. As the sunlight exposure time increases degradation percentage increases. Undoped ZnO nanoparticles decolorized the solution in 210 min with 81.93%. Ce (0.03 wt%) doped ZnO nanoparticles decolorized the solution in 120 min with 92.62 % efficiency.

## References

[1] Daksh Daksh and Yadvendra Kumar Agrawal 2016 Rare Earth-Doped Zinc Oxide Nanostructures. *Rev. Nanosci. Nanotechnol.* 5: 1–27

[2] Aisah N, Gustiono D, Fauzia V, Sugihartono I and Nuryadi R 2017 Synthesis and Enhanced Photocatalytic Activity of Ce-Doped Zinc Oxide Nanorods by Hydrothermal Method. *IOP Conf. Series*: *Mater. Sci. Eng.* 172: 012037

[3] Clament Sagaya Selvam N, Judith Vijaya J and John Kennedy L 2014 Effect of Ce doping on structural, optical and photocatalytic properties of ZnO nano-structures. *J. Nanosci. Nanotechnol.* 14: 2317–2324

[4] Behzad Shahmoradi, Soga K, Ananda S, Somashekar R and Byrappa K 2010 Modification of neodymium-doped ZnO hybrid nanoparticles under mild hydrothermal conditions. *Nanoscale* 2: 1160–1164

[5] Phuruangrat A, Thongtem T, Satchawan S and Thongtem S 2018 Photocatalytic activity of rugby-like Nd-doped ZnO particles activated by ultraviolet. *Dig. J. Nanomater. Biostruct.* 13: 625–630

[6] Theivarasu C and Indumathi T 2016 Effect of rare earth metal ion Ce3+ on the structural, optical and magnetic properties of ZnO nanoparticles synthesized by the co-precipitation method. *J. Mater. Sci. Mater. Electron.* https://doi.org/10.1007/s10854-016-5971-6

[7] Richter H, Wang Z P and Ley L 1981 The one phonon Raman spectrum in microcrystalline silicon. *Solid State Commun.* 39: 625–629

[8] Bilel Chouchene, Tahar Ben Chaabane, Lavinia Balan, Emilien Girot, Kevin Mozet, Ghouti Medjahdi and Raphaël Schneider 2016 High performance Ce-doped ZnO nanorods for sunlight-driven photocatalysis, *Beilstein J. Nanotechnol.* 7: 1338–1349

[9] Bomilaa R, Srinivasana S, Venkatesanb A, Bharathc B and Perinbam K 2017 Structural, optical and antibacterial activity studies of Ce-doped ZnO nanoparticles prepared by wet-chemical method, *Mater. Res. Innovat.* 1433–075X

[10] Chin Boon Onga, Law Yong Ngb and Abdul Wahab Mohammad 2018 A review of ZnO nanoparticles as solar photocatalysts: Synthesis, mechanisms and applications *Renew. Sustain. Energy Rev.* 81: 536–551

[11] Labhane P K, Patle1 L B, Huse V R and Sonawane G H 2018 Synthesis of Ce doped ZnO nanoparticles coupled with graphene oxide as efficient photocatalyst for the degradation of dye under day light, *2nd International Conference on Condensed Matter and Applied Physics (ICC 2017) AIP Conf. Proc.* 1953, 030008-1–030008-4

[12] Xinyu Zhang, Jiaqian Qin, Yanan Xue, Pengfei Yu, Bing Zhang, Limin Wang and Riping Liu 2010 Effect of aspect ratio and surface defects on the photocatalytic activity of ZnO nanorods. *Sci. Rep.* 4: 4596